

# Multivariate Probabilistic Forecasting of Intraday Electricity Prices using Normalizing Flows

Eike Cramer<sup>a,b</sup>, Dirk Witthaut<sup>c,d</sup>, Alexander Mitsos<sup>e,a,f</sup>, Manuel Dahmen<sup>a,\*</sup>

<sup>a</sup> Forschungszentrum Jülich GmbH, Institute of Energy and Climate Research, Energy Systems Engineering (IEK-10), Jülich 52428, Germany

<sup>b</sup> RWTH Aachen University Aachen 52062, Germany

<sup>c</sup> Forschungszentrum Jülich GmbH, Institute of Energy and Climate Research, Systems Analysis and Technology Evaluation (IEK-STE), Jülich 52428, Germany

<sup>d</sup> Institute for Theoretical Physics, University of Cologne, 50937 Köln, Germany

<sup>e</sup> JARA-ENERGY, Jülich 52425, Germany

<sup>f</sup> RWTH Aachen University, Process Systems Engineering (AVT.SVT), Aachen 52074, Germany

Electricity is traded on various markets with different time horizons and regulations. Short-term trading becomes increasingly important due to higher penetration of renewables. In Germany, the intraday electricity price typically fluctuates around the day-ahead price of the EPEX spot markets in a distinct hourly pattern. This work proposes a probabilistic modeling approach that models the intraday price difference to the day-ahead contracts. The model captures the emerging hourly pattern by considering the four 15 min intervals in each day-ahead price interval as a four-dimensional joint distribution. The resulting nontrivial, multivariate price difference distribution is learned using a normalizing flow, i.e., a deep generative model that combines conditional multivariate density estimation and probabilistic regression. The normalizing flow is compared to a selection of historical data, a Gaussian copula, and a Gaussian regression model. Among the different models, the normalizing flow identifies the trends most accurately and has the narrowest prediction intervals. Notably, the normalizing flow is the only approach that identifies rare price peaks. Finally, this work discusses the influence of different external impact factors and finds that, individually, most of these factors have negligible impact. Only the immediate history of the price difference realization and the combination of all input factors lead to notable improvements in the forecasts.

**Keywords:** Electricity price forecasting; probabilistic forecasting; deep learning; multivariate modeling

## 1 Introduction

The liberalization of the European electricity market into the EPEX spot markets has introduced the auction-based day-ahead market and the continuously traded intraday market (Mayer and Trück, 2018). The hourly day-ahead auction market is cleared on the day before delivery. Afterward, the continuous 15 min interval intraday markets aim to reduce the balance requirements by enabling short-term changes to delivery and consumption commitments and react to ramping of supply and demand (Ocker and Ehrhart, 2017; Kiesel and Paraschiv, 2017; Koch and Hirth, 2019; European Power Exchange, 2021; Bublitz et al., 2019). The increasing penetration of renewable electricity sources with low marginal cost (Sensfuß et al., 2008) causes intraday prices to become more volatile (Viehmann, 2017). Thus, electricity price forecasting (EPF) (Weron, 2014) for the intraday market becomes increasingly difficult (Lago et al., 2021; Jedrzejewski et al., 2022) as the forecasts have to account for the

inherent uncertainty of intermittent renewable electricity supply and human interaction on the continuous market (Mayer and Trück, 2018; Bublitz et al., 2019).

A promising approach to address the uncertainty in EPF uses probabilistic forecasting models that predict a distribution of possible realizations instead of a single point forecast (Zhang et al., 2003; Nowotarski and Weron, 2018). The quantitative knowledge of the uncertainty allows the market participants to develop different strategies considering the range of possible outcomes and to derive more effective bidding strategies (Nowotarski and Weron, 2018). Established approaches for probabilistic forecasting include prediction intervals (Zhang et al., 2003; Serinaldi, 2011; Jónsson et al., 2014; Uniejewski and Weron, 2021) and density forecasts (Huurman et al., 2012; Panagiotelis and Smith, 2008; Andrade et al., 2017; Narajewski and Ziel, 2020b). Other works use ensemble forecasts (Narajewski and Ziel, 2020b) or propose combina-

\*Manuel Dahmen, Forschungszentrum Jülich GmbH, Institute of Energy and Climate Research, Energy Systems Engineering (IEK-10), Jülich 52428, Germany  
E-mail: m.dahmen@fz-juelich.de

tions of deterministic and probabilistic approaches (Marcjasz et al., 2020).

The majority of probabilistic EPF papers utilize univariate modeling approaches (Nowotarski and Weron, 2018), i.e., the models predict single time steps in a step-by-step fashion and consider the correlation between time steps via the autoregressive components. Alternatively, multivariate models predict sequences in multi-step forecasting (Panagiotelis and Smith, 2008; Ziel and Weron, 2018). For instance, Panagiotelis and Smith (2008) use a multivariate student-t distribution model for intraday prices in Australia. In a study on deterministic forecasting models, Ziel and Weron (2018) report on the advantages of using a multivariate approach for day-ahead EPF.

Most of the previously mentioned literature on probabilistic EPF only considers the day-ahead markets (Lago et al., 2021). A notable exception is presented by Andrade et al. (2017) who perform probabilistic forecasting for both day-ahead and intraday markets.

The literature on intraday EPF generally addresses the intraday prices as a stand-alone prediction problem without considering the relation to the day-ahead prices. However, separating the intraday EPF from the day-ahead prices ignores the connection between the two markets, where the intraday market mainly serves to make adjustments to the fixed day-ahead contracts (Kiesel and Paraschiv, 2017; Koch and Hirth, 2019). Consequently, the intraday price follows the day-ahead price trend. Furthermore, the adjustments react to the ramping of supply and demand, which leads to steadily increasing or decreasing prices in the four intraday trading intervals of each day-ahead trading interval (Kiesel and Paraschiv, 2017). Thus, there is a distinct hourly fluctuation of the intraday prices around the day-ahead prices that averages to the day-ahead price (Kiesel and Paraschiv, 2017; Han et al., 2022). This work proposes a modeling approach for intraday electricity prices based on the special relationship between the two electricity markets. Assuming that the intraday EPF is performed short-term, i.e., after the day-ahead price is set, the intraday price is modeled via the difference between the two market prices. Furthermore, the hourly increasing or decreasing pattern of the four 15 min intervals of each day-ahead price interval are captured using a multivariate joint distribution.

The proposed four-dimensional distribution of price differences is modeled using normalizing flows (Dinh et al., 2017; Papamakarios et al., 2021), a

non-parametric, i.e., fully data-driven, distribution model. Normalizing flows learn complex distributions without a priori assumptions about the data and can include external impact factors for probabilistic regression (Winkler et al., 2019; Rasul et al., 2021). For scenario generation of other energy time series, such as renewable electricity generation and electricity demand, normalizing flows have already shown promising results (Dumas et al., 2022; Cramer et al., 2022a,b; Arpogaus et al., 2021). The forecasting performance of the normalizing flow is evaluated in comparison to an informed selection of historical data, a Gaussian copula, and a multivariate Gaussian regression.

The remainder of this work is organized as follows: Section 2 introduces the four-dimensional price difference modeling approach and highlights the advantages of multivariate modeling over the traditional univariate approach. Section 3 introduces the different multivariate probabilistic models and discusses relevant external input factors. Section 4 applies the different distribution modeling approaches to learn the four-dimensional conditional distribution and discusses the impact of each external input factor via an empirical study. Finally, Section 5 concludes this work.

## 2 Electricity price analysis

This Section first describes the used data sets. Second, an approach for multivariate modeling of intraday electricity prices is proposed. Finally, the Section compares a univariate and a multivariate sampling approach for the price difference vector using assessment scores for multivariate probabilistic forecasting.

### 2.1 Data description

The majority of electricity is traded on the auction-based day-ahead market, while the intraday market is primarily used to make short-term adjustments to the previously submitted bids (Han et al., 2022). The intraday contracts are negotiated between the producers and the consumers on different time horizons and for different periods. Thus, different prices occur for the same intraday trading interval (Mayer and Trück, 2018; Ocker and Ehrhart, 2017). As an indicator of the intraday electricity prices, the market operators release indices of volume-weighted averages (European Power Exchange, 2021). This work uses the ID<sub>3</sub> index, i.e., the index reflecting the volume-weighted average price of the last

three hours before delivery, as it is the most commonly used indicator (European Power Exchange, 2021; Bublitz et al., 2019). The data set considered in this work is the day-ahead and ID<sub>3</sub> price time series recorded over the years of 2018 and 2019 provided by the Fraunhofer-Institut für Solare Energiesysteme ISE (2022). The renewable electricity production forecasts and actual production values for the same time frame are taken from ENTSO-E Transparency Platform (2022). All renewable electricity time series are recorded in 15 min intervals. Note that the electricity price data from 2020 and 2021 shows atypical behavior due to the COVID-19 pandemic (Michał Narajewski, 2020; Badesa et al., 2021) and is, therefore, not included.

## 2.2 Hourly price difference vectors

The volume of electricity traded on the day-ahead and the intraday markets exemplifies the relationship between the two markets. In 2019, the volume of day-ahead trades was 501.6 TWh, and the intraday trades amounted to 83.2 TWh (European Power Exchange (EPEX SPOT), 2020). These numbers explicate how traders primarily use the day-ahead market and the intraday market only to make adjustments to the previously submitted bids. Intraday trades address ramping of supply and demand within the day-ahead trading intervals and compensate for forecast errors of demand and renewable electricity supply (Kiesel and Paraschiv, 2017; Spodniak et al., 2021). In particular, the ramping of large suppliers and consumers leads to a distinct pattern of increasing or decreasing intraday prices within each day-ahead trading interval (Kiesel and Paraschiv, 2017). For instance, a scheduled ramp up of electricity supply results in an undersupply in the first 15 minutes and an oversupply in the last 15 minutes of the respective hour, which leads to higher prices in the first 15 minutes and lower prices in the last 15 minutes, respectively. Thus, the hour-wise constant day-ahead contracts lead to hourly patterns in the 15 min intraday prices (Kiesel and Paraschiv, 2017; Han et al., 2022).

Figure 1 shows the trends of the day-ahead and the ID<sub>3</sub> index price on September 10<sup>th</sup>, 2019. As indicated by Kiesel and Paraschiv (2017), the average ID<sub>3</sub> price within each hour is close to the respective day-ahead price. Furthermore, the ID<sub>3</sub> price is either increasing or decreasing within the respective day-ahead trading intervals. Figure 2 shows the average daily day-ahead and intraday prices in 2018 and 2019, i.e., each step represents the average price interval over the two years. The profiles

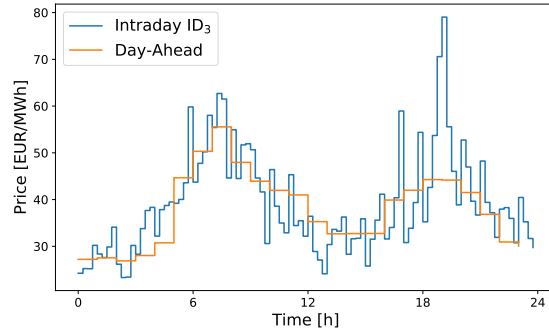


**Fig. 1.** Example of daily profiles of day-ahead and ID<sub>3</sub> price trends on September 10<sup>th</sup>, 2019. EPEX spot price data from Fraunhofer-Institut für Solare Energiesysteme ISE (2022).

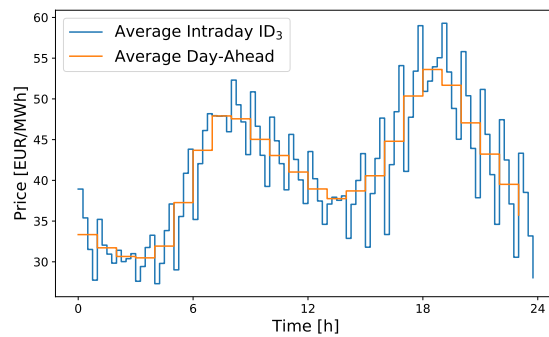


**Fig. 2.** Average daily profiles of day-ahead and ID<sub>3</sub> price trends of 2018 and 2019. EPEX spot price data from Fraunhofer-Institut für Solare Energiesysteme ISE (2022).

support the observations made in Figure 1 and by Kiesel and Paraschiv (2017): First, the  $ID_3$  index fluctuates around the day-ahead auction price. Second, Figure 2 highlights that the distinct hourly patterns of either increasing or decreasing steps appear systematically. Exceptions of this pattern only appear at local minima and maxima of the day-ahead price. In summary, the relationship between the day-ahead and the intraday markets as primary and adjustment markets leads to a distinct hourly pattern of intraday price fluctuations around the day-ahead prices.

The proposed modeling approach for the  $ID_3$  price index aims to capture this fluctuational pattern. Since the intraday market is used for adjustments to the day-ahead market, the difference between the two price time series represents the characteristics of the intraday market. Assuming that the prediction takes place after the day-ahead auction has been settled and the day-ahead prices are known, the  $ID_3$  price index can be described via the sum of the day-ahead price and the difference between the two price time series. Furthermore, the hourly pattern of fluctuations is captured by modeling the four steps of price differences in each day-ahead trading interval as a four-dimensional vector. For a given hour  $t$  the price difference vector  $\Delta ID_3$  then reads:

$$\Delta ID_3(t) = \begin{bmatrix} ID_3^{00}(t) - DA(t) \\ ID_3^{15}(t) - DA(t) \\ ID_3^{30}(t) - DA(t) \\ ID_3^{45}(t) - DA(t) \end{bmatrix} \quad (1)$$

The four dimensions each describe the difference between intraday and day-ahead price for a 15 min interval. The superscripts 00, 15, 30, 45 indicate the starting minutes of the four intraday trading intervals.

### 2.3 Price difference vector analysis

To showcase the advantage of the multivariate modeling approach, this Section first highlights the strong correlation between the four price difference time steps in each day-ahead trading interval by showing the Pearson correlation and then compares a univariate and a multivariate sampling approach to highlight how the multivariate approach better captures the correlations between the time steps.

Table 1 shows the Pearson correlation of the four dimensions in the joint distribution of price differences. The correlations between neighboring time steps are high and, thus, highlight the strong corre-

**Tab. 1.** Pearson correlation within the 4D- $\Delta ID_3$  distribution (see Equation (2)). Price data from Fraunhofer-Institut für Solare Energiesysteme ISE (2022).

|                    | $\Delta ID_3^{00}$ | $\Delta ID_3^{15}$ | $\Delta ID_3^{30}$ | $\Delta ID_3^{45}$ |
|--------------------|--------------------|--------------------|--------------------|--------------------|
| $\Delta ID_3^{00}$ | 1.00               | 0.77               | 0.41               | 0.09               |
| $\Delta ID_3^{15}$ | 0.77               | 1.00               | 0.74               | 0.46               |
| $\Delta ID_3^{30}$ | 0.41               | 0.74               | 1.00               | 0.83               |
| $\Delta ID_3^{45}$ | 0.09               | 0.46               | 0.83               | 1.00               |

lation between the time steps within each day-ahead trading interval.

To confirm that the multivariate approach captures the correlation shown in Table 1 better than the classical univariate approach, two different approaches of univariate and multivariate selection of historical data are compared using scoring metrics for multivariate probabilistic forecasts. Figure 2 shows a strong dependency of the average realization on the hour of the day. The multivariate selection is based on this observation and randomly selects historical realizations of the hourly price difference intervals that occurred during the same hour of the day. Similarly, the univariate selection approach randomly selects values that occurred during the same 15 min interval and combines the selections into four-dimensional samples. Both approaches randomly select price differences from 2018 and 2019 with the exception of July 2019, which is set aside as a test set.

Unlike point forecasts, probabilistic forecasts cannot be evaluated by residual metrics such as the mean-square-error or the mean-absolute-error. Instead, probabilistic forecasts are typically evaluated in terms of reliability and sharpness (Nowotarski and Weron, 2018). Here, reliability describes whether the realization lies within certain prediction intervals. Sharpness analyses the tightness of the prediction intervals, i.e., how close the lower and upper boundaries of the prediction intervals are together (Nowotarski and Weron, 2018). A good probabilistic forecast should be both reliable and sharp to avoid missing the realization and avoid large prediction intervals that carry little information.

To evaluate the different sampling approaches, this work uses the energy score (Gneiting and Raftery, 2007; Pinson and Girard, 2012) and the variogram score (Scheuerer and Hamill, 2015). The energy score (Gneiting et al., 2008; Pinson and Girard, 2012) is a widely applied metric for multistep

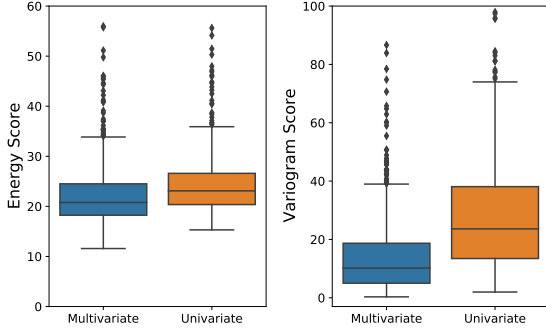


**Fig. 3.** Box plots (Waskom, 2021) of the energy score (Gneiting and Raftery, 2007; Pinson and Girard, 2012) and variogram score (Scheuerer and Hamill, 2015) distributions of historical data selected using univariate and multivariate approaches. Price data from 2018 and 2019 (Fraunhofer-Institut für Solare Energiesysteme ISE, 2022) and test set in July 2019.

probabilistic forecasts that assesses how close the prediction samples are to the realizations and how diverse the samples are:

$$ES = \frac{1}{N} \sum_{s=1}^N \|\mathbf{x} - \hat{\mathbf{x}}_s\|_2 - \frac{1}{2N^2} \sum_{s=1}^N \sum_{s'=1}^N \|\hat{\mathbf{x}}_s - \hat{\mathbf{x}}_{s'}\|_2$$

Here,  $\mathbf{x}$  is the realized  $ID_3$  price-vector, i.e., the actual realization from the test set,  $\hat{\mathbf{x}}_s$  are sample vectors drawn from the predicted distributions,  $N$  is the number of samples, and  $\|\cdot\|_2$  is the 2-norm. The variogram score (Scheuerer and Hamill, 2015) aims to assess whether a multivariate forecast correctly describes the correlation between the individual time steps:

$$VS = \frac{1}{N} \sum_{t=1}^{\hat{T}} \sum_{t'=1}^{\hat{T}} \left( |x_t - x_{t'}|^\gamma - \frac{1}{N} \sum_{s=1}^N |\hat{x}_t^s - \hat{x}_{t'}^s|^\gamma \right)^2$$

Here,  $x_t$  are the realized  $ID_3$  price time steps,  $\hat{x}_t$  are time steps of samples from the predicted  $ID_3$  distribution,  $\hat{T} = 4$  is the quarter hour interval,  $N$  is the number of samples,  $\gamma$  is the variogram order (typically  $\gamma = 0.5$  (Scheuerer and Hamill, 2015)), and  $|\cdot|$  denotes the absolute value. Both energy score and variogram score are negatively oriented metrics, i.e., lower values indicate better performance (Scheuerer and Hamill, 2015; Pinson and Girard, 2012).

Figure 3 shows box plots (Waskom, 2021) of the energy score and the variogram score distributions of the univariate and the multivariate selection approaches applied to each day-head trading interval

of the test month, respectively. The multivariate approach yields lower values for energy scores and variogram scores and, thus, indicates better agreement with the realizations. In particular, the variogram score highlights that the univariate selection fails to represent the correct correlation between the time steps whereas the multivariate approach captures the hourly pattern. In conclusion, the results in Figure 3 confirm that the multivariate approach is better suited to describe the price difference distribution than a univariate approach. In the following, the term historical selection refers to the multivariate selection of historical data.

### 3 Multivariate probabilistic forecasting of electricity price differences

This Section introduces the different modeling approaches for the conditional probability distribution of the electricity price difference vector in Equation (1). Furthermore, this Section discusses relevant external factors included in the probabilistic regression.

#### 3.1 Multivariate probabilistic regression

The realizations of the hourly price difference vector in Equation (1) follow a four-dimensional joint distribution:

$$\Delta ID_3 \sim p_{\Delta ID_3}(\Delta ID_3) \quad (2)$$

Here,  $p_{\Delta ID_3}(\Delta ID_3)$  is the probability density function (PDF) of the vector-valued random variable  $\Delta ID_3$ . As the realizations of the price difference distribution are assumed to be influenced by known external factors  $\mathbf{y}$ , the proposed modeling approach includes these external factors to form a conditional distribution:

$$\Delta ID_3 \sim p_{\Delta ID_3|\mathbf{y}}(\Delta ID_3|\mathbf{y}) \quad (3)$$

To model the conditional probability distribution of price differences described by Equation (3), this work uses the following four approaches: (1) conditional normalizing flows (Winkler et al., 2019), (2) the informed selection of historical data presented in Section 2 to serve as a benchmark for the other models, (3) Gaussian copulas with quantile regression (Pinson et al., 2009), and (4) multivariate Gaussian regression (Dillon et al., 2017).

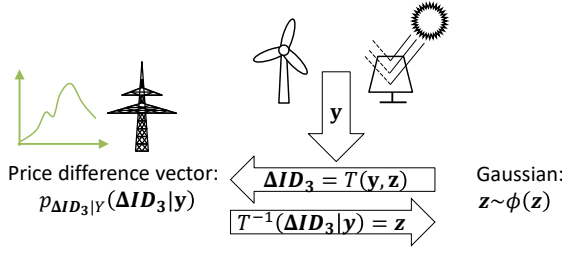


**Fig. 4.** Sketch of the normalizing flow modeling approach. The horizontal arrows indicate the transformation of Gaussian samples  $\mathbf{z} \sim \phi(\mathbf{z})$  to samples of the price difference vector  $\Delta \mathbf{ID}_3$  and vice versa. The external factors  $\mathbf{y}$ , e.g., renewable electricity forecast errors, are considered as additional inputs to the transformation  $T$ .

Normalizing flows are non-parametric distribution models that model high-dimensional complex distributions as an invertible neural network transformation  $T$ , with inverse  $T^{-1}$ , of a multivariate standard Gaussian  $\phi(\mathbf{z})$  (Dinh et al., 2017; Papamakarios et al., 2021). Utilizing the change of variables formula, normalizing flows describe the conditional PDF  $p_{X|Y}(\mathbf{x}|\mathbf{y})$  of a multivariate random variable  $X$  with realizations  $\mathbf{x}$  and inputs  $\mathbf{y}$  explicitly (Papamakarios et al., 2021; Winkler et al., 2019):

$$p_{X|Y}(\mathbf{x}|\mathbf{y}) = \phi(T^{-1}(\mathbf{x}, \mathbf{y})) |\det \mathbf{J}_{T^{-1}}(\mathbf{x}, \mathbf{y})| \quad (4)$$

Here,  $\mathbf{J}_{T^{-1}}$  is the Jacobian of the inverse transformation. Normalizing flows make no assumptions about the data structure and distribution. Thus, by using sufficiently expressive transformations, normalizing flows can model any distribution (Papamakarios et al., 2021). To sample from a normalizing flow, first, samples are drawn from the multivariate Gaussian  $\hat{\mathbf{z}}_i \sim \phi(\mathbf{z})$ . Second, the samples and the conditional inputs are transformed using the forward form of the invertible neural network:

$$\hat{\mathbf{x}}_i = T(\hat{\mathbf{z}}_i, \hat{\mathbf{y}} = \text{const.}) \quad \forall i = 1, 2, \dots, N$$

Here,  $\hat{\mathbf{y}} = \text{const.}$  are the external inputs at the respective time. Figure 4 shows a sketch of the conditional normalizing flow modeling scheme. For the implementation of the invertible neural network, this work uses the real non-volume preserving transformation (RealNVP) (Dinh et al., 2017).

The Gaussian copula is a well-established method to describe multivariate distributions with nontrivial correlations between the individual dimensions.

The basic approach relies on transforming samples from a uniform distribution via an estimated inverse cumulative distribution function (CDF). In forecasting applications, the inverse CDF is estimated via interpolation of quantile forecasts from quantile regression. For a detailed introduction on the combination with quantile regression, we refer the interested reader to Pinson et al. (2009). The present work uses the quantile regression in Seabold and Perktold (2010).

Finally, the multivariate Gaussian regression uses neural networks to predict the mean vector  $\mu_X$  and the covariance matrix  $\Sigma_X$  of the multivariate Gaussian as a function of the conditional inputs  $\mathbf{y}$  (Dillon et al., 2017):

$$p_{X|Y}(\mathbf{x}|\mathbf{y}) = \mathcal{N}_{X|Y}(\mathbf{x}; \mu_X(\mathbf{y}), \Sigma_X(\mathbf{y})) \quad (5)$$

As the covariance matrix is symmetric, the neural network only needs to predict a lower-triangular version of  $\Sigma_X(\mathbf{y})$  (Dillon et al., 2017). The predicted mean and covariance can then be used to sample from the Gaussian distribution parameterized by the predicted values.

In all models, the electricity price difference vector  $\Delta \mathbf{ID}_3$  takes the role of the random variable  $X$ , and the external factors are the conditional inputs  $Y$ . For every realization of the external factors  $\mathbf{y}$ , the models allow sampling from the electricity price difference vector distribution  $\Delta \hat{\mathbf{ID}}_3 \sim p_{\Delta \mathbf{ID}_3}$  as described for the normalizing flow above.

### 3.2 External factors

The realizations of both the day-ahead and the intraday prices are influenced by external factors. These external factors include any information that informs about the realizations of the electricity price differences. Examples of external factors for day-ahead and intraday prices include the electricity demand, supply from renewable electricity, and the time of the delivery (Wolff and Feuerriegel, 2017; Naumzik and Feuerriegel, 2021). However, the proposed model considers the difference between the two market prices, which alleviates the impact of some external factors and amplifies the impact of others. In particular, the impact of the forecasted total electricity demand and the forecasted total renewable electricity supply is already considered in the day-ahead market and has little influence on the price differences (Kiesel and Paraschiv, 2017; Spodniak et al., 2021; Han et al., 2022). The intraday markets are used to adjust the previously submitted bids on the day-ahead market,

which are based on forecasts. Thus, the differences are mostly impacted by the forecasting errors for demand and renewables (Kiesel and Paraschiv, 2017; Han et al., 2022). The renewable forecast errors are computed as the difference between the realization and the forecast:

$$\Delta P_t^{RE} = P_t^{RE} - \hat{P}_t^{RE} \quad RE \in \{\text{Solar}, \text{Wind}\}$$

Here,  $P_t^{RE}$  is the actual generation,  $\hat{P}_t^{RE}$  is the day-ahead generation forecast.

Another important external factor for the fluctuation of the intraday prices is the ramping of solar electricity generation in the morning and at night, which leads to large changes in solar power supply within single day-ahead trading intervals (Koch and Hirth, 2019). Wolff and Feuerriegel (2017) and Ocker and Ehrhart (2017) find that the relation of conventional and renewable electricity impacts the realizations of both day-ahead and intraday prices. To investigate whether the relation also impacts the price difference, the quotient of conventional and renewable power in the grid is included as an external factor:

$$P_t^{\text{rel}} = \frac{P_t^{\text{conventional}}}{P_t^{\text{renewable}}}$$

Figure 2 suggests that the increments of the day-ahead price, i.e., the difference between one hour and the next, have a substantial impact on the direction (increasing or decreasing) and the intensity of the hourly fluctuation. For increasing or decreasing day-ahead prices, the hourly fluctuation shows increasing or decreasing patterns, respectively (Han et al., 2022). Furthermore, larger increments appear to induce more significant fluctuations and vice versa. For local minimum and maximum peak hours in the day-ahead price, Figure 2 shows no distinct trend of the fluctuation.

Figure 2 also indicates that the realizations of the price differences depend on the time of the day. Thus, the proposed model includes this time dependency by including a trigonometric encoding of the hour of the day (Moon et al., 2019). Neither the day of the week nor the month of the year significantly impacts the price differences. The supplementary material contains further details of the impact of the time of the day, day of the week, and month of the year.

Narajewski and Ziel (2020a) and Han et al. (2022) state that the day-ahead markets in Germany are weak-form efficient, i.e., the recent history of day-ahead prices does not inform on future realizations, whereas for intraday prices, there is an advantage

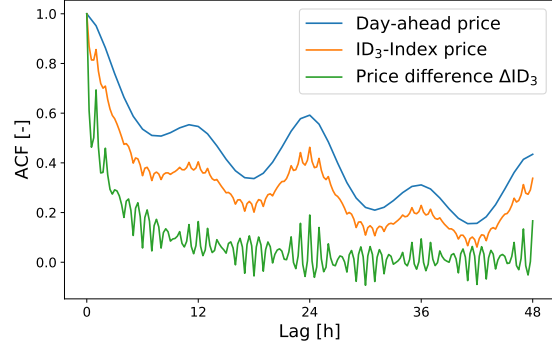


**Fig. 5.** Pearson autocorrelation (ACF) of day-ahead price (“Day-ahead price”), ID<sub>3</sub> index (“ID<sub>3</sub>-Index price”), and difference between the two time series (“Price difference  $\Delta\text{ID}_3$ ”) with time lag of 0 to 48 h. Price data in 2018 and 2019 (Fraunhofer-Institut für Solare Energiesysteme ISE, 2022).

from including the most recent value in the prediction. To evaluate the impact of prior realizations on the price difference, Figure 5 shows the Pearson autocorrelation function (ACF) of the day-ahead price, the intraday price, and the difference between the two time series. The ACF of the price difference drops quickly and continues to fluctuate around low values that are significantly lower compared to the day-ahead ACF and the intraday ACF. However, the first hour still shows high ACF values and is, thus, included in the external inputs.

Table 2 lists the Pearson correlation of all considered external factors with the 4 dimensions of the price difference vector in Equation (1). The Pearson correlation indicates the highest dependency on the immediate history of the price difference vector. Most other considered factors show moderate to low correlation factors. However, the low correlation does not indicate that there is no value in including those external factors in the probabilistic forecast as Pearson correlations describe only the linear correlations of the mean. In the numerical experiments section of this work, we perform an empirical evaluation of the influence of the different external factors.

Note that some of the considered external factors are not known until the realization of the intraday price. For instance, the exact forecast errors are unknown at the forecasting time. Hence, this work considers these factors as a feasibility study for the multivariate modeling approach and postpones the discussion about the timing of the probabilistic forecast.

**Tab. 2.** Pearson correlation between the price difference dimensions  $\Delta\text{ID}_3$  and conditional input factors. Q00, ..., Q45 indicate the for 15 min intervals in each day-ahead trading interval. Price data from [Fraunhofer-Institut für Solare Energiesysteme ISE \(2022\)](#) and renewables data from [ENTSO-E \(ENTSO-E Transparency Platform, 2022\)](#).

| External factors               | $\Delta\text{ID}_3^{00}$ | $\Delta\text{ID}_3^{15}$ | $\Delta\text{ID}_3^{30}$ | $\Delta\text{ID}_3^{45}$ |
|--------------------------------|--------------------------|--------------------------|--------------------------|--------------------------|
| Day Ahead Auction Price        | -0.03                    | -0.05                    | -0.05                    | -0.04                    |
| Day Ahead Increments -1        | -0.44                    | -0.16                    | 0.14                     | 0.31                     |
| Day Ahead Increments +1        | 0.38                     | 0.10                     | -0.22                    | -0.42                    |
| cos hour encoding              | 0.11                     | 0.03                     | -0.04                    | -0.10                    |
| sin hour encoding              | 0.01                     | 0.00                     | 0.02                     | -0.01                    |
| $\Delta\text{ID}_3^{00}(t-1h)$ | 0.72                     | 0.55                     | 0.28                     | 0.05                     |
| $\Delta\text{ID}_3^{15}(t-1h)$ | 0.70                     | 0.69                     | 0.51                     | 0.31                     |
| $\Delta\text{ID}_3^{30}(t-1h)$ | 0.49                     | 0.67                     | 0.69                     | 0.56                     |
| $\Delta\text{ID}_3^{45}(t-1h)$ | 0.24                     | 0.53                     | 0.70                     | 0.67                     |
| Solar Forecast Error Q00       | -0.20                    | -0.23                    | -0.21                    | -0.15                    |
| Solar Forecast Error Q15       | -0.20                    | -0.24                    | -0.23                    | -0.17                    |
| Solar Forecast Error Q30       | -0.20                    | -0.24                    | -0.24                    | -0.18                    |
| Solar Forecast Error Q45       | -0.20                    | -0.24                    | -0.24                    | -0.19                    |
| Wind Forecast Error Q00        | -0.28                    | -0.36                    | -0.38                    | -0.32                    |
| Wind Forecast Error Q15        | -0.28                    | -0.36                    | -0.39                    | -0.33                    |
| Wind Forecast Error Q30        | -0.28                    | -0.37                    | -0.39                    | -0.33                    |
| Wind Forecast Error Q45        | -0.28                    | -0.36                    | -0.39                    | -0.34                    |
| Absolute solar Q00             | -0.11                    | -0.06                    | -0.01                    | 0.06                     |
| Absolute solar Q15             | -0.09                    | -0.06                    | -0.02                    | 0.04                     |
| Absolute solar Q30             | -0.07                    | -0.05                    | -0.03                    | 0.02                     |
| Absolute solar Q45             | -0.05                    | -0.05                    | -0.04                    | 0.00                     |
| Relative fossil Q00            | 0.05                     | 0.04                     | 0.04                     | 0.04                     |
| Relative fossil Q15            | 0.04                     | 0.03                     | 0.05                     | 0.05                     |
| Relative fossil Q30            | 0.03                     | 0.03                     | 0.05                     | 0.06                     |
| Relative fossil Q45            | 0.03                     | 0.03                     | 0.05                     | 0.06                     |

## 4 Numerical experiments

This section investigates whether the different modeling approaches can describe the four-dimensional price difference distribution. Each model is trained on the data set from 2018 and 2019 (Fraunhofer-Institut für Solare Energiesysteme ISE, 2022), where the month of July 2019 is again set aside as a test set. The  $24\text{ h} \times 31\text{-day}$  test set results in 744 test intervals. Note that July 1st, 2019, was a Monday. To preprocess the data and avoid complications from the heavy-tailed distributions (Han et al., 2022), the data is transformed using the probability integral transform discussed in Uniejewski et al. (2017), which renders the data in a Gaussian form. The normalizing flow and the Gaussian regression are trained via log-likelihood maximization over 500 epochs with a batch size of 128 using the python-based machine-learning library TensorFlow version 2.8.0 (Abadi and Agarwal, 2015). The Gaussian copula uses the quantile regression in the statsmodels python library (Seabold and Perktold, 2010). For details on the implementation of the models, see the supplementary material. One hundred samples are drawn for each hour in the test set and used to compute the different metrics outlined in Section 2.

### 4.1 Prediction intervals

This Section analyzes the forecasted distributions by investigating the 50% and 90% prediction intervals. The intervals are estimated by computing the respective quantiles for each time step and then adding the day-ahead price of the given hour to reverse the difference in Equation (1).

Figure 6 shows the predicted mean, the 50% and 90% prediction intervals, and the intraday price realization for the first four days in the test month of July 2019. The Figure shows the results estimated from probabilistic forecasts from the normalizing flow (top), the selection of historical data (second from top), the Gaussian copula (third from top), and the Gaussian regression (bottom). For the presented test days, the normalizing flow encloses the realization for most of the time steps, and the forecast mean appears to identify the realized trends well, with very few exceptions. The selection of historical data reflects the trends moderately well and portrays wider prediction intervals compared to the normalizing flow. The Gaussian copula and Gaussian regression often fail to identify the correct trends and do not fit the realizations as tightly as the normalizing flow. In particular,

**Tab. 3.** Percentage of realizations within 50% and 90% prediction intervals (PI).

|                  | PI 50% | PI 90% |
|------------------|--------|--------|
| Normalizing Flow | 59.4%  | 93.5%  |
| Historical       | 62.1%  | 95.5%  |
| Copula           | 61.6%  | 96.0%  |
| Gaussian         | 54.9%  | 90.2%  |

the Gaussian copula results in extensive prediction intervals that show vast peaks for the 90% prediction interval. Compared to the other approaches, the normalizing flow performs significantly better in identifying the trends and keeping narrow prediction intervals. Overall, the normalizing flow yields the sharpest prediction intervals while the Gaussian copula shows low sharpness.

On the first day in the days shown in Figure 6, there is a significant peak in the ID<sub>3</sub> price realization. This type of extreme event may occur due to unforeseen incidences in the markets, such as unplanned changes in the operation of large consumers or suppliers. Notably, the normalizing flow is the only approach that captures this peak. The supplementary material shows the prediction intervals for other peak days in the test month that confirm the normalizing flows’ ability to capture the price peaks.

Table 3 shows the percentage of time steps in the test set that lie within the 50% and 90% prediction interval, respectively. All approaches show conservative results for both prediction intervals, i.e., the actual percentage of realizations within the prediction intervals is higher than the selected probability. Thus, all approaches yield reliable prediction intervals.

In summary, the normalizing flow shows the best results with sharp prediction interval presented in Figure 6 and reliable results in Table 3. The selection of historical data shows surprisingly good results but shows poor sharpness in the prediction intervals due to the missing conditional input information. The Gaussian copula results in prediction intervals with poor sharpness and extreme peaks that are likely a result of a poor quantile regression of the tails of the price difference distribution. By overestimating the tails in the inverse CDF, the Gaussian copula samples a higher share of outliers than the actual distribution. The high reliability indicated in Table 3 comes at the cost of poor sharpness. Finally, the Gaussian regression has to predict a total of 14 values for the mean vector and

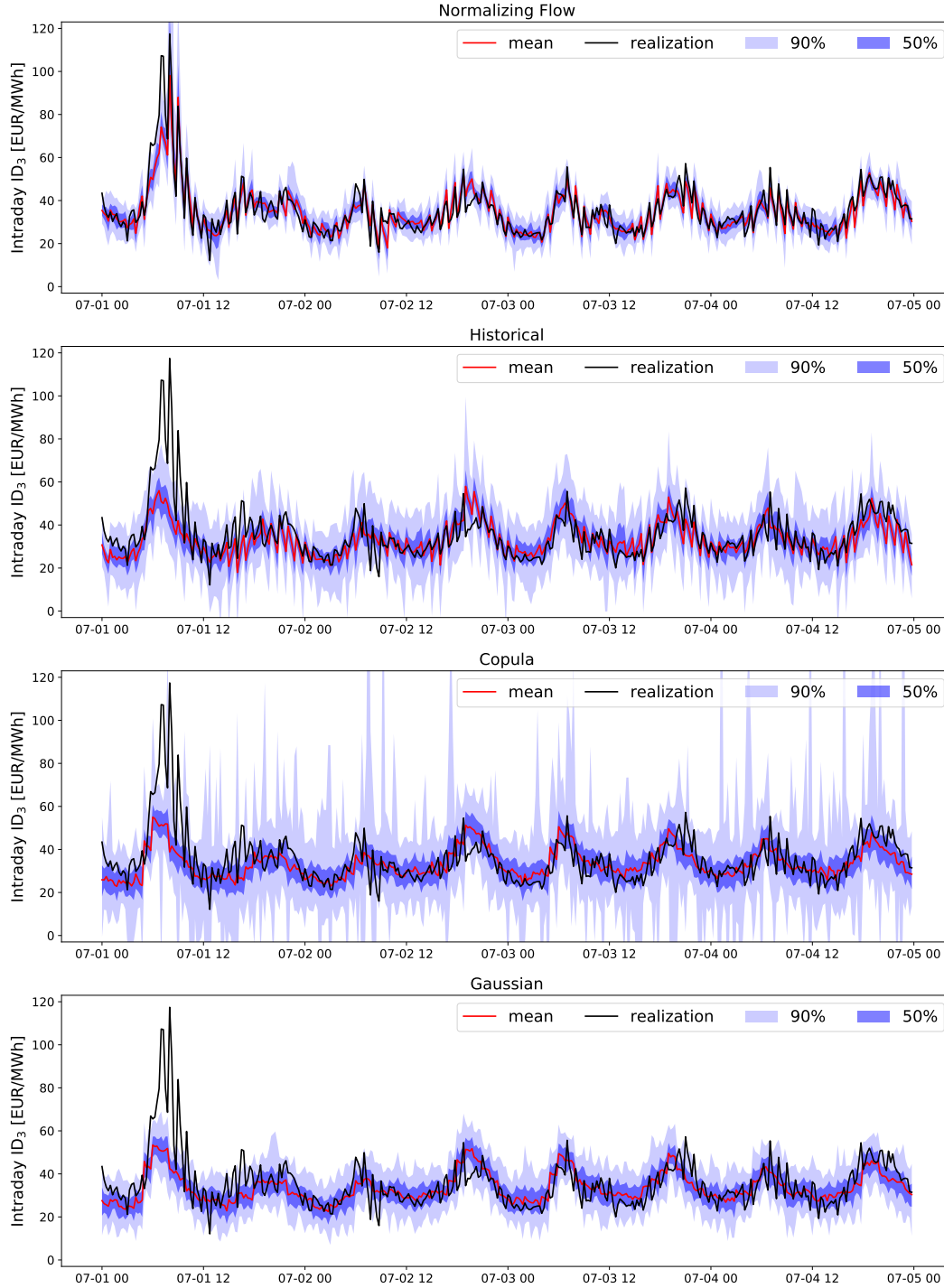


**Fig. 6.** Predicted mean, prediction intervals of 50% and 90%, and realization for the first five days of July 2019 estimated from probabilistic forecasts from the normalizing flow (top) the informed selection of historical data (second from top), the Gaussian copula (third from top), and the Gaussian regression (bottom). Note the truncated y-axis for the Gaussian copula. Training data from 2018 and 2019 ([Fraunhofer-Institut für Solare Energiesysteme ISE, 2022](#)). Results generated with all conditional inputs shown in Table 2.

a lower-triangular covariance matrix (Dillon et al., 2017). Likely, this number is too high to achieve good fits in the regression model and, instead, the training regresses to constant outputs.

## 4.2 Energy and variogram score

Figure 7 shows the energy score for each model and each hour of the test month (left), as well as box plots of the overall energy score distributions (right). The Gaussian regression performs only marginally better than the historical selection. As shown in Figure 6, the Gaussian regression struggles to identify the correct trends, and the historical selection shows wider prediction intervals, i.e., both approaches show weaknesses that lead to an increase in the energy score in different ways. The Gaussian copula shows significantly worse results than the other forecasting models. As already observed in Figure 6, the Gaussian copula results in extensive prediction intervals and fails to identify the intraday price patterns. Thus, the large energy scores in Figure 7 confirm the qualitative observations from Figure 6. Finally, the normalizing flow shows the lowest energy score, i.e., it provides the most reliable predictions while maintaining sharp prediction intervals. The excellent performance of the normalizing flows stems from a correct identification of the trends and maintaining narrow prediction intervals. Furthermore, the normalizing flow generates a diverse set of samples.

In general, the energy scores over time in the case of all methods show rare incidences of extreme price peaks, e.g., on the first day and at the beginning of the last quarter of the month. Notably, however, the normalizing flow shows the best approximation of these extreme events, e.g., for the price peak on the first day of the test month shown in Figure 6 and the other peak days shown in the supplementary material.

Next, the variogram score is used to compare whether the different models can identify the correlation between the dimensions. Figure 8 shows the variogram score for each model and each hour of the test month (left), as well as box plots of the overall distributions (right). Note that the y-axis of the right of Figure 8 is truncated to allow for better visualization of the distributions. Similar to the energy score results, the normalizing flow shows the best results while the Gaussian regression performs approximately equal to the historical selection. The Gaussian copula appears to miss large parts of the correlation and shows the worst variogram scores. The flexibility of the normalizing flow allowed the

model to learn the correlation between the four time steps in the price difference vector better than any other considered approach.

In conclusion, the flexibility of the normalizing flow can describe the non-trivial distribution of the considered price differences, as highlighted by both the energy scores and the variogram scores for the test month. Furthermore, the combination with external impact factors leads to a significant improvement over the historical selection. Meanwhile, both Gaussian copula and Gaussian regression result in erroneous trends and inflated prediction intervals.

## 4.3 Significance of external factors

The Pearson correlations in Table 2 indicate a moderate dependency of the price differences on many of the considered external factors but a strong correlation with the prior realization of the price difference vector. Up to this point, however, it remains unclear whether these correlations translate into better forecasting performance. Figure 9 shows box plots of the energy score and variogram score distributions over the test month for samples generated using the normalizing flow with different sets of external factors in comparison to the selection of historical data. Note the truncated y-axis to highlight the majority parts of the distributions.

The energy score results highlight that most of the individual external factors do not improve the probabilistic forecasts compared to the selection of historical data. The encoding of time (“Time”), the renewables forecast errors (“Forecast Errors”), the absolute solar power generation (“Solar Rampling”), and the relation of fossil electricity to renewables (“Relative Fossil”) all show approximately the same energy score as the historical data. Meanwhile, the day-ahead price increments (“Increments”) show a moderate improvement, and the previous realization of the price difference vector (“Previous Interval”) results in lower energy scores. Notably, the combination of all external factors (“All”) achieves the lowest energy scores.

The variogram score confirms the observations from the energy score. Except for the increments (“Increments”) and the previous realizations (“Previous Interval”), all inputs lead to approximately equal or slightly worse results compared to the informed historical selection. Again, the previous realizations show the strongest impact, and the combination of all external factors leads to the lowest variogram score overall.

In conclusion, the previous realization of the price difference vector has by far the strongest impact on

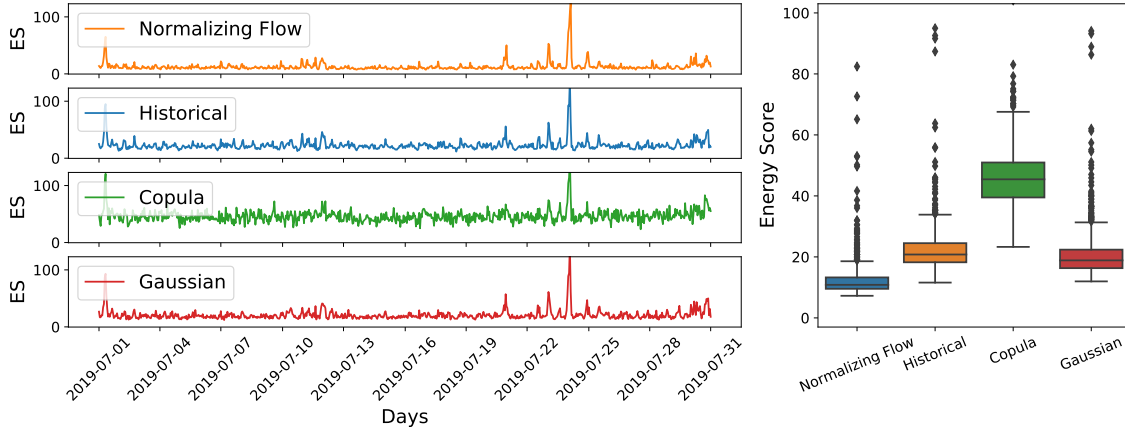


**Fig. 7.** Energy score (Gneiting et al., 2008; Pinson and Girard, 2012) of the normalizing flow (“Normalizing Flow”), the selection of historical data (“Historical”), the Gaussian copula (“Copula”), and the Gaussian regression (“Gaussian”) for each hour in test month of July 2019 (left) and box plot (Waskom, 2021) of the overall distribution for each model (right). Training data from 2018 and 2019 (Fraunhofer-Institut für Solare Energiesysteme ISE, 2022). Conditional inputs as shown in Table 2.

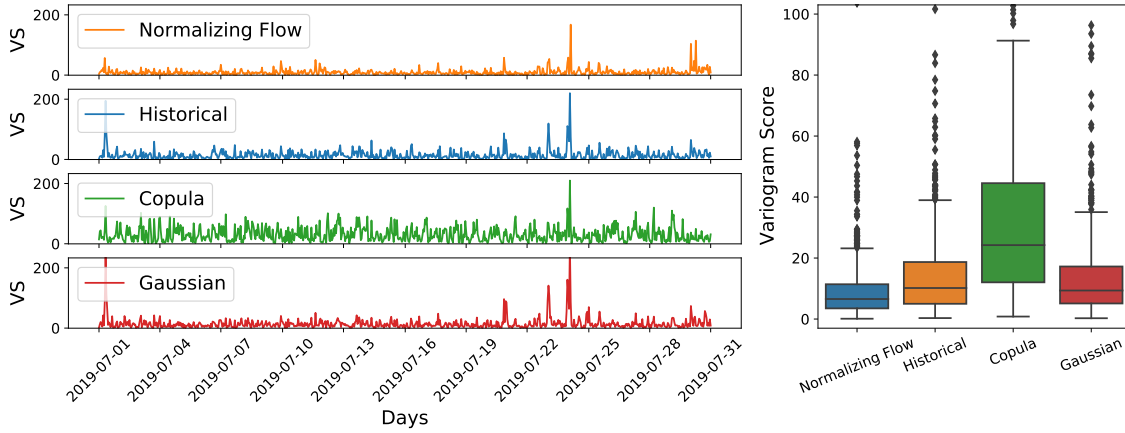


**Fig. 8.** Variogram score (Scheuerer and Hamill, 2015) of the normalizing flow (“Normalizing Flow”), the selection of historical data (“Historical”), the Gaussian copula (“Copula”), and the Gaussian regression (“Gaussian”) for each hour in test month of July 2019 (left) and box plot (Waskom, 2021) of the overall distribution for each model (right). Training data from 2018 and 2019 (Fraunhofer-Institut für Solare Energiesysteme ISE, 2022). Conditional inputs as shown in Table 2.

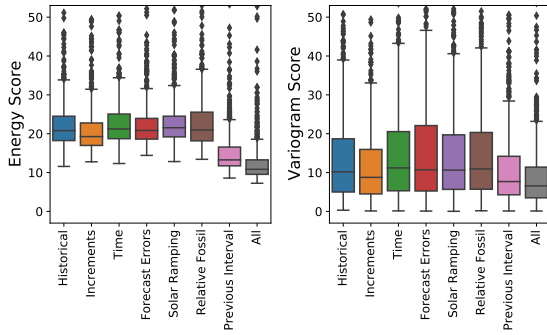


**Fig. 9.** Energy score (Gneiting et al., 2008; Pinson and Girard, 2012) and variogram score (Scheuerer and Hamill, 2015) of normalizing flow predictions using different sets of external factors. Note the truncated y-axis. Training data from 2018 and 2019 (Fraunhofer-Institut für Solare Energiesysteme ISE, 2022) and July 2019 as test set.

the probabilistic forecasts, as already indicated by the high Pearson correlation in Table 2. However, the normalizing flow can still extract additional information from the remaining external factors while also learning to ignore irrelevant information.

Narajewski and Ziel (2020a) and Han et al. (2022) argue that the intraday markets are not efficient in the sense of the “efficient-market hypothesis” as there are strong relations between the current and previous realizations. The improved results of the normalizing flow from using previous realizations as input factors confirm the observation of high dependency on previous realizations.

The analysis in this section shows promising results that indicate valuable density forecasts of the price difference vector by the normalizing flow. Both the Gaussian copula and the Gaussian regression show weaknesses and fail to improve on the results of the informed historical selection suggesting they are not suitable prediction methods. Figure 9 shows that only the knowledge of the realizations in the previous hour poses an advantage over using the informed selection of historical data. Hence, lead times of multiple hours rescind the advantage of the normalizing flow over the informed historical selection. In conclusion, the normalizing flow yields high-quality density forecasts for short lead times. If less information is available, the selection of historical price differences based on the hour of the day appears to be sufficient.

## 5 Conclusion

This work proposes a modeling approach for probabilistic forecasting of intraday electricity prices in the German EPEX spot market. The novel approach captures the strong relation between day-ahead and intraday prices by assuming fixed day-ahead prices and predicting the difference between the two price time series. Furthermore, the model captures the hourly patterns of fluctuation of the intraday prices around the day-ahead prices by considering each day-ahead trading interval as a four-dimensional joint distribution.

The non-parametric distribution model called normalizing flow is used to learn the proposed four-dimensional distribution of price differences and includes external input factors to form a conditional density forecast. The proposed model yields a complete end-to-end approach for multivariate density estimation and probabilistic regression that does not require any a priori assumptions about the data.

Compared to a selection of historical data and other multivariate probabilistic models, namely the Gaussian copula and multivariate Gaussian regression, the normalizing flow returns both the most reliable and sharpest predictions. In summary, the normalizing flow best identifies the trends of the intraday prices and shows the narrowest prediction intervals.

The empirical comparison of different impact factors highlights that the combination of multiple input factors leads to the lowest energy scores. Among the different impact factors, the prior realizations of the price difference vector result in the largest improvement, while other subsets of impact factors perform approximately equal to the historical selection. The good performance of using the previous price differences confirms the strong dependency found in the statistical analysis by Han et al. (2022).

In conclusion, the analysis shows promising results that indicate valuable price difference density forecasts. Future studies on forecasting the difference between intraday and day-ahead prices should focus on identifying significant impact factors considering their attainability at different points in time. For instance, the short-term  $2\frac{1}{4}$  h renewable forecasts could be valuable substitutes for the currently used exact realizations to estimate the forecast errors.

## Acknowledgements

We gratefully acknowledge Johannes Kruse (FZ-Jülich IEK-STE), Julius Trebbien (FZ-Jülich IEK-STE), and Leonard Rydin Gorjão (Department of Computer Science, OsloMet) for the discussion about the concepts and the importance of different impact factors. This work was performed as part of the Helmholtz School for Data Science in Life, Earth and Energy (HDS-LEE) and received funding from the Helmholtz Association of German Research Centres.

## Nomenclature

| Symbol   | Description  |
|--|--|
| $N$  | Number of samples  |
| $P_t^{\text{conventional}}$  | Conventional electricity in the grid                           |
| $P_t^{\text{renewable}}$   | Renewable electricity in the grid                              |
| $P_t^{\text{rel}}$   | Relation of conventional and renewable electricity in the grid |
| $P_t^{RE}$   | Renewable electricity from $RE \in \{\text{Solar, Wind}\}$     |
| $\hat{P}_t^{RE}$   | Forecast of renewable electricity                              |
| $\Delta P_t^{RE}$  | Forecast error of renewable electricity                        |
| $T$  | Invertible neural network                                      |
| $\mathbf{J}_{T-1}$   | Jacobian of $T^{-1}$   |
| $\hat{T}$  | Day-ahead trading interval $\hat{T} = 4$                       |
| $x_t$  | Value at time step $t$   |
| $\hat{x}_t$  | Sample at time step $t$  |
| $\mathbf{x}, \mathbf{y}$   | Data vector  |
| $\hat{\mathbf{z}}$   | Gaussian sample  |
| $\hat{\mathbf{x}}, \hat{\mathbf{y}}$                                     | Sample of data vector  |
| $\mathbf{y}$   | External input factors   |
| $\text{ID}_3$  | Intraday price   |
| $\text{ID}_3^{00}, \text{ID}_3^{15}, \text{ID}_3^{30}, \text{ID}_3^{45}$ | Quarter hour steps of intraday prices                          |
| DA   | Day-ahead price  |
| $\Delta \text{ID}_3$   | 4D vector of price difference                                  |
| $\phi$   | Multivariate standard Gaussian                                 |

| Symbol   | Description   |
|--|---|
| $\mathcal{N}_{X Y}(\mathbf{x}; \boldsymbol{\mu}_X(\mathbf{y}), \boldsymbol{\Sigma}_X(\mathbf{y}))$ | Conditional Gaussian distribution                           |
| $p_{X Y}(\mathbf{x} \mathbf{y})$   | Conditional PDF of $X$ given $Y$                            |
| $p_{\Delta \text{ID}_3 Y}(\Delta \text{ID}_3 \mathbf{y})$  | Conditional PDF of $\Delta \text{ID}_3$ given $Y$           |
| $\mathcal{N}_{X Y}$  | Gaussian distribution with moments predicted via inputs $Y$ |
| $\boldsymbol{\mu}_X(\mathbf{y})$   | Neural network mean value predictor                         |
| $\boldsymbol{\Sigma}_X(\mathbf{y})$  | Neural network covariance matrix value predictor            |
| $\gamma$   | Variogram order (typically $\gamma = 0.5$ )                 |

## Bibliography

- Abadi, M. and Agarwal, A. (2015). TensorFlow: Large-scale machine learning on heterogeneous systems. <https://www.tensorflow.org/>. Accessed on 08-08-2021.
- Andrade, J. R., Filipe, J., Reis, M., and Bessa, R. J. (2017). Probabilistic price forecasting for day-ahead and intraday markets: Beyond the statistical model. *Sustainability*, 9(11):1990.
- Arpogaus, M., Voß, M., Sick, B., Nigge-Uricher, M., and Dürr, O. (2021). Probabilistic short-term low-voltage load forecasting using bernstein-polynomial normalizing flows. In *ICML 2021 Workshop on Tackling Climate Change with Machine Learning*, virtual.
- Badesa, L., Strbac, G., Magill, M., and Stojkovska, B. (2021). Ancillary services in Great Britain during the COVID-19 lockdown: A glimpse of the carbon-free future. *Applied Energy*, 285:116500.
- Bublitz, A., Keles, D., Zimmermann, F., Fraunholz, C., and Fichtner, W. (2019). A survey on electricity market design: Insights from theory and real-world implementations of capacity remuneration mechanisms. *Energy Economics*, 80:1059–1078.
- Cramer, E., Mitsos, A., Tempone, R., and Dahmen, M. (2022a). Principal component density estimation for scenario generation using normalizing flows. *Data-Centric Engineering*, 3:e7.
- Cramer, E., Paeleke, L., Mitsos, A., and Dahmen, M. (2022b). Normalizing flow-based day-ahead

- wind power scenario generation for profitable and reliable delivery commitments by wind farm operators. *arXiv preprint arXiv:2204.02242*.
- Dillon, J. V., Langmore, I., Tran, D., Brevdo, E., Vasudevan, S., Moore, D., Patton, B., Alemi, A., Hoffman, M., and Saurous, R. A. (2017). Tensorflow distributions. *arXiv preprint arXiv:1711.10604*.
- Dinh, L., Sohl-Dickstein, J., and Bengio, S. (2017). Density estimation using Real NVP. In *5th International Conference on Learning Representations, ICLR 2017, Toulon, France, April 24-26, 2017, Conference Track Proceedings*. OpenReview.net.
- Dumas, J., Wehenkel, A., Lanaspese, D., Cornélusse, B., and Sutera, A. (2022). A deep generative model for probabilistic energy forecasting in power systems: Normalizing flows. *Applied Energy*, 305:117871.
- ENTSO-E Transparency Platform (2022). ENTSO-E Transparency Platform. <https://transparency.entsoe.eu/>. Accessed: 2022-03-01.
- European Power Exchange (2021). EPEX SPOT documentation. <http://www.epexspot.com/en/extras/download-center/documentation>. Accessed: 2021-05-30.
- European Power Exchange (EPEX SPOT) (2020). Annual report 2019. [https://www.epexspot.com/sites/default/files/download\\_center\\_files/Epex-spot-2019\\_200703\\_Planche.pdf](https://www.epexspot.com/sites/default/files/download_center_files/Epex-spot-2019_200703_Planche.pdf). Accessed: 2021-05-30.
- Fraunhofer-Institut für Solare Energiesysteme ISE (2022). Energy Charts. <https://www.energy-charts.info>. Accessed: 2022-03-01.
- Gneiting, T. and Raftery, A. E. (2007). Strictly proper scoring rules, prediction, and estimation. *Journal of the American Statistical Association*, 102(477):359–378.
- Gneiting, T., Stanberry, L. I., Grimit, E. P., Held, L., and Johnson, N. A. (2008). Assessing probabilistic forecasts of multivariate quantities, with an application to ensemble predictions of surface winds. *Test*, 17(2):211–235.
- Han, C., Hilger, H., Mix, E., Böttcher, P. C., Reyers, M., Beck, C., Witthaut, D., and Gorjão, L. R. (2022). Complexity and persistence of price time series of the european electricity spot market. *PRX Energy*, 1(1):013002.
- Huurman, C., Ravazzolo, F., and Zhou, C. (2012). The power of weather. *Computational Statistics & Data Analysis*, 56(11):3793–3807.
- Jedrzejewski, A., Lago, J., Marcjasz, G., and Weron, R. (2022). Electricity price forecasting: The dawn of machine learning. *IEEE Power and Energy Magazine*, 20(3):24–31.
- Jónsson, T., Pinson, P., Madsen, H., and Nielsen, H. A. (2014). Predictive densities for day-ahead electricity prices using time-adaptive quantile regression. *Energies*, 7(9):5523–5547.
- Kiesel, R. and Paraschiv, F. (2017). Econometric analysis of 15-minute intraday electricity prices. *Energy Economics*, 64:77–90.
- Koch, C. and Hirth, L. (2019). Short-term electricity trading for system balancing: An empirical analysis of the role of intraday trading in balancing germany’s electricity system. *Renewable and Sustainable Energy Reviews*, 113:109275.
- Lago, J., Marcjasz, G., De Schutter, B., and Weron, R. (2021). Forecasting day-ahead electricity prices: A review of state-of-the-art algorithms, best practices and an open-access benchmark. *Applied Energy*, 293:116983.
- Marcjasz, G., Uniejewski, B., and Weron, R. (2020). Probabilistic electricity price forecasting with narx networks: Combine point or probabilistic forecasts? *International Journal of Forecasting*, 36(2):466–479.
- Mayer, K. and Trück, S. (2018). Electricity markets around the world. *Journal of Commodity Markets*, 9:77–100.
- Michał Narajewski, F. Z. (2020). Changes in electricity demand pattern in europe due to COVID-19 shutdowns. *IAEE Energy Forum*, pages 44–47.
- Moon, J., Park, S., Rho, S., and Hwang, E. (2019). A comparative analysis of artificial neural network architectures for building energy consumption forecasting. *International Journal of Distributed Sensor Networks*, 15(9):1550147719877616.
- Narajewski, M. and Ziel, F. (2020a). Econometric modelling and forecasting of intraday electricity prices. *Journal of Commodity Markets*, 19:100107.

- Narajewski, M. and Ziel, F. (2020b). Ensemble forecasting for intraday electricity prices: Simulating trajectories. *Applied Energy*, 279:115801.
- Naumzik, C. and Feuerriegel, S. (2021). Forecasting electricity prices with machine learning: Predictor sensitivity. *International Journal of Energy Sector Management*, 15(1):157–172.
- Nowotarski, J. and Weron, R. (2018). Recent advances in electricity price forecasting: A review of probabilistic forecasting. *Renewable and Sustainable Energy Reviews*, 81:1548–1568.
- Ocker, F. and Ehrhart, K.-M. (2017). The “German Paradox” in the balancing power markets. *Renewable and Sustainable Energy Reviews*, 67:892–898.
- Panagiotelis, A. and Smith, M. (2008). Bayesian density forecasting of intraday electricity prices using multivariate skew t distributions. *International Journal of Forecasting*, 24(4):710–727.
- Papamakarios, G., Nalisnick, E., Rezende, D. J., Mohamed, S., and Lakshminarayanan, B. (2021). Normalizing flows for probabilistic modeling and inference. *Journal of Machine Learning Research*, 22(57):1–64.
- Pinson, P. and Girard, R. (2012). Evaluating the quality of scenarios of short-term wind power generation. *Applied Energy*, 96:12–20.
- Pinson, P., Madsen, H., Nielsen, H. A., Papaefthymiou, G., and Klöckl, B. (2009). From probabilistic forecasts to statistical scenarios of short-term wind power production. *Wind Energy: An International Journal for Progress and Applications in Wind Power Conversion Technology*, 12(1):51–62.
- Rasul, K., Sheikh, A.-S., Schuster, I., Bergmann, U. M., and Vollgraf, R. (2021). Multivariate probabilistic time series forecasting via conditioned normalizing flows. In *International Conference on Learning Representations*.
- Scheuerer, M. and Hamill, T. M. (2015). Variogram-based proper scoring rules for probabilistic forecasts of multivariate quantities. *Monthly Weather Review*, 143(4):1321–1334.
- Seabold, S. and Perktold, J. (2010). Statsmodels: Econometric and statistical modeling with python. In *Proceedings of the 9th Python in Science Conference*, pages 92–96, Austin, TX.
- Sensfuß, F., Ragwitz, M., and Genoese, M. (2008). The merit-order effect: A detailed analysis of the price effect of renewable electricity generation on spot market prices in germany. *Energy policy*, 36(8):3086–3094.
- Serinaldi, F. (2011). Distributional modeling and short-term forecasting of electricity prices by generalized additive models for location, scale and shape. *Energy Economics*, 33(6):1216–1226.
- Spodniak, P., Ollicka, K., and Honkapuro, S. (2021). The impact of wind power and electricity demand on the relevance of different short-term electricity markets: The nordic case. *Applied Energy*, 283:116063.
- Uniejewski, B. and Weron, R. (2021). Regularized quantile regression averaging for probabilistic electricity price forecasting. *Energy Economics*, 95:105121.
- Uniejewski, B., Weron, R., and Ziel, F. (2017). Variance stabilizing transformations for electricity spot price forecasting. *IEEE Transactions on Power Systems*, 33(2):2219–2229.
- Viehmann, J. (2017). State of the German short-term power market. *Zeitschrift für Energiewirtschaft*, 41(2):87–103.
- Waskom, M. L. (2021). Seaborn: statistical data visualization. *Journal of Open Source Software*, 6(60):3021.
- Weron, R. (2014). Electricity price forecasting: A review of the state-of-the-art with a look into the future. *International Journal of Forecasting*, 30(4):1030–1081.
- Winkler, C., Worrall, D., Hoogeboom, E., and Welling, M. (2019). Learning likelihoods with conditional normalizing flows. *arXiv preprint arXiv:1912.00042*.
- Wolff, G. and Feuerriegel, S. (2017). Short-term dynamics of day-ahead and intraday electricity prices. *International Journal of Energy Sector Management*, 11:557–573.
- Zhang, L., Luh, P. B., and Kasiviswanathan, K. (2003). Energy clearing price prediction and confidence interval estimation with cascaded neural networks. *IEEE Transactions on Power Systems*, 18(1):99–105.

- Ziel, F. and Weron, R. (2018). Day-ahead electricity price forecasting with high-dimensional structures: Univariate vs. multivariate modeling frameworks. *Energy Economics*, 70:396–420.

# Multivariate Probabilistic Forecasting of Intraday Electricity Prices using Normalizing Flows

Eike Cramer<sup>a,b</sup>, Dirk Witthaut<sup>c,d</sup>, Alexander Mitsos<sup>e,a,f</sup>, Manuel Dahmen<sup>a,\*</sup>

<sup>a</sup> Forschungszentrum Jülich GmbH, Institute of Energy and Climate Research, Energy Systems Engineering (IEK-10), Jülich 52425, Germany

<sup>b</sup> RWTH Aachen University Aachen 52062, Germany

<sup>c</sup> Forschungszentrum Jülich GmbH, Institute of Energy and Climate Research, Systems Analysis and Technology Evaluation (IEK-STE), Jülich 52428, Germany

<sup>d</sup> Institute for Theoretical Physics, University of Cologne, 50937 Köln, Germany

<sup>e</sup> JARA-ENERGY, Jülich 52425, Germany

<sup>f</sup> RWTH Aachen University, Process Systems Engineering (AVT.SVT), Aachen 52074, Germany

## 1 Time dependency

Figures 1, 2, and 3 show the dependency of the price difference vector on the hour of the day, the day of the week, and the month of the year, respectively. Notably, only the hour of the day appears to have a significant impact on the realizations. This also indicates a similar behavior of the price differences for weekdays and weekends.

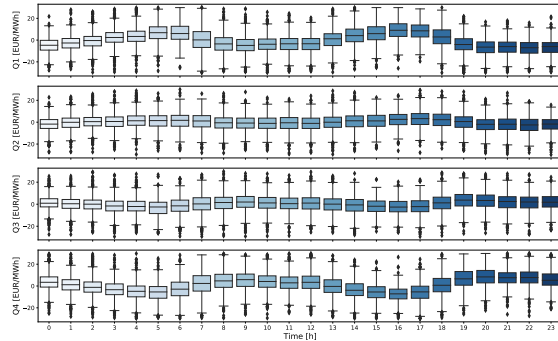


**Fig. 1.** Box plots of distribution of price difference as function of hour of the day.

## 2 Additional analysis of Winkler score

The Winkler score (Winkler, 1972; Gneiting and Raftery, 2007) is a well-established test to investigate reliability and sharpness:

$$\text{WS} = \begin{cases} \delta_t & x_t \in [\hat{L}_t^\alpha, \hat{U}_t^\alpha] \\ \delta_t + \frac{2}{1-\alpha} (\hat{U}_t^\alpha - x_t) & x_t \geq \hat{U}_t^\alpha \\ \delta_t + \frac{2}{1-\alpha} (x_t - \hat{L}_t^\alpha) & x_t \leq \hat{L}_t^\alpha \end{cases}$$

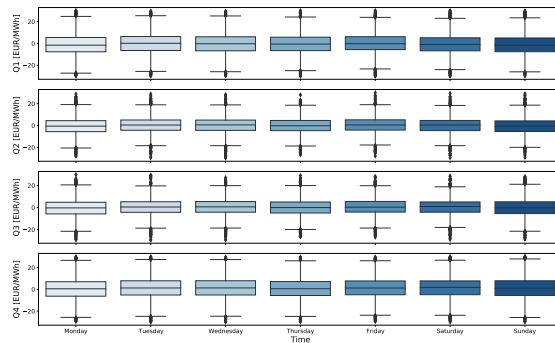


**Fig. 2.** Box plots of distribution of price difference as function of day of the week.

Here,  $x_t$  is the time step,  $\hat{L}_t^\alpha$  and  $\hat{U}_t^\alpha$  are the lower and upper bound of the confidence interval with probability  $\alpha$ , respectively. The term  $\delta_t$  indicates the width of the predicted confidence interval:

$$\delta_t = \hat{U}_t^\alpha - \hat{L}_t^\alpha$$

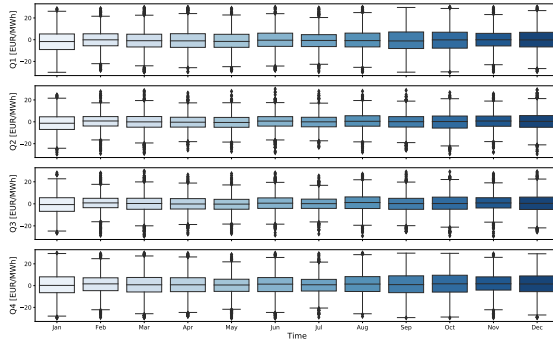
The Winkler score is a negatively oriented score, i.e., lower values indicate better performance.

Figure 4 shows the distributions of Winkler scores over the full month of July 2019 for each of the probabilistic models and over  $\alpha$  values between 0.0 and 0.9. Overall, the normalizing flow shows the best results.

## 3 ANN structures

The Gaussian regression uses a fully-connected neural network with one hidden layer, 32 neurons, and ‘tanh’ activation. The output layer has 14 neurons to describe the four-dimensional mean and the lower triangular covariance matrix implemented in TensorFlow-probability (Dillon et al., 2017). The

\*Manuel Dahmen, Forschungszentrum Jülich GmbH, Institute of Energy and Climate Research, Energy Systems Engineering (IEK-10), Jülich 52425, Germany  
E-mail: m.dahmen@fz-juelich.de



**Fig. 3.** Box plots of distribution of price difference as function of month of the year.

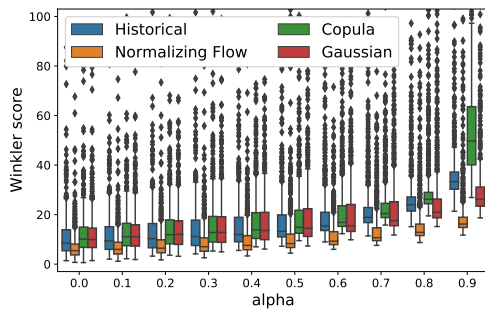


**Fig. 4.** Winkler score (Winkler, 1972; Gneiting and Raftery, 2007) over confidence interval width  $\alpha$  for the different models and the historical data. Full distribution of scores over the month of July 2019.

neuron that output the mean have no activation and the neurons that output the covariance matrix use ‘softmax’ activation to ensure strict positivity.

The normalizing flow uses the affine coupling layer implementation in (Dinh et al., 2017). The full model uses four affine coupling layers with fully connected conditioner models. The conditioner models have two hidden layers with ‘ReLU’ activation and four neurons per layer.

## 4 Prediction intervals on extreme peaks

Figure 5 shows the predicted mean, the prediction intervals of 50% and 90%, and the realization between July 21<sup>st</sup> and July 26<sup>th</sup> of 2019. Similar to the prediction intervals shown in the main part of the paper, the results confirm that the normalizing flow results in the narrowest prediction intervals and is

the only approach that captures the extreme price peaks.

## Bibliography

Dillon, J. V., Langmore, I., Tran, D., Brevdo, E., Vasudevan, S., Moore, D., Patton, B., Alemi, A., Hoffman, M., and Saurous, R. A. (2017). Tensorflow distributions. *arXiv preprint arXiv:1711.10604*.

Dinh, L., Sohl-Dickstein, J., and Bengio, S. (2017). Density estimation using Real NVP. In *5th International Conference on Learning Representations, ICLR 2017, Toulon, France, April 24-26, 2017, Conference Track Proceedings*. Open-Review.net.

Fraunhofer-Institut für Solare Energiesysteme ISE (2022). Energy Charts. <https://www.energy-charts.info>. Accessed: 2022-03-01.

Gneiting, T. and Raftery, A. E. (2007). Strictly proper scoring rules, prediction, and estimation. *Journal of the American Statistical Association*, 102(477):359–378.

Winkler, R. L. (1972). A decision-theoretic approach to interval estimation. *Journal of the American Statistical Association*, 67(337):187–191.

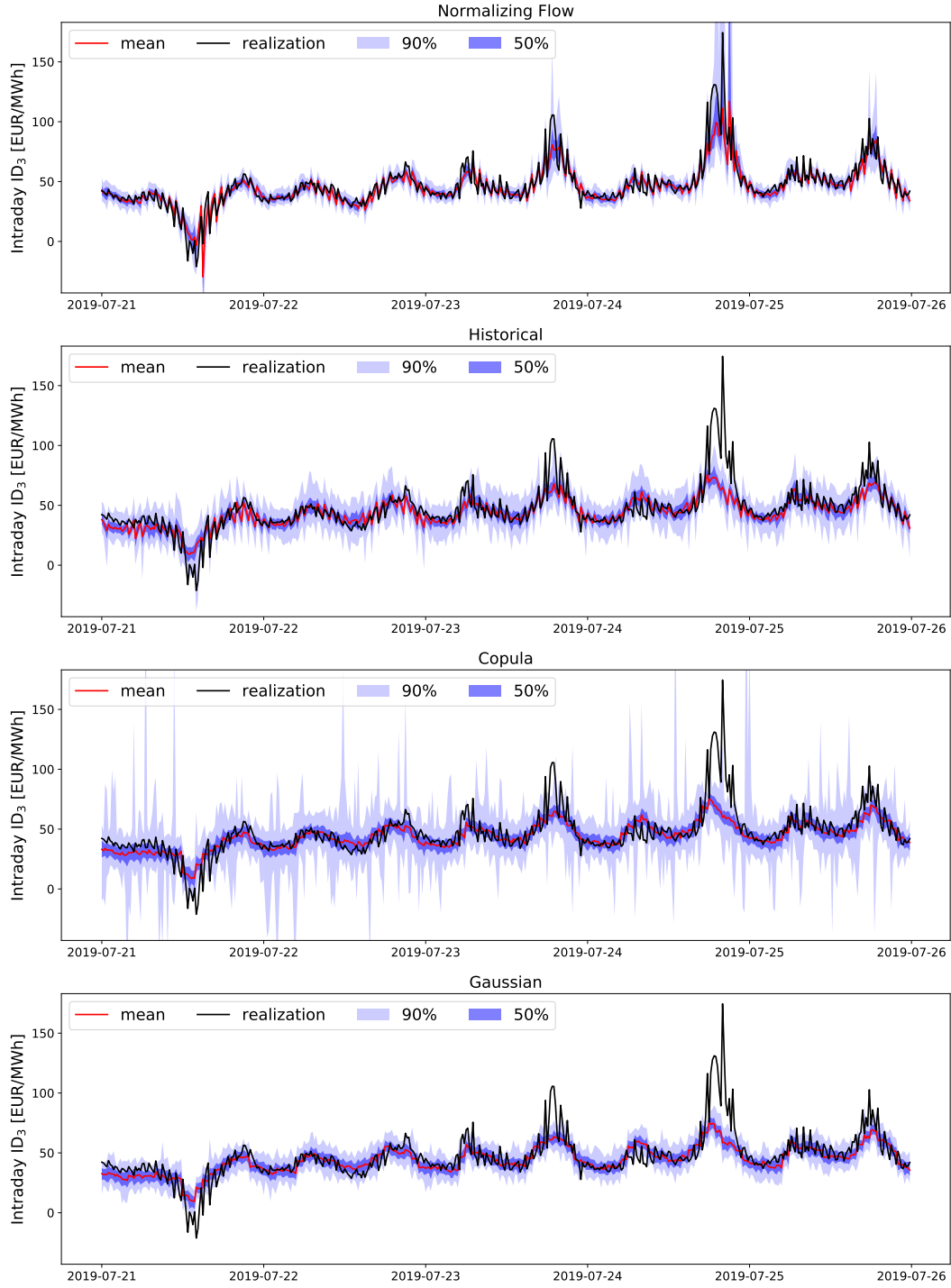


**Fig. 5.** Predicted mean, prediction intervals of 50% and 90%, and realization between July 21<sup>st</sup> and July 26<sup>th</sup> of 2019 estimated from the probabilistic forecasts from the normalizing flow (top), the selection of historical data (second from top), the Gaussian copula (third from top), and the Gaussian regression (bottom). Note the truncated y-axis for the Gaussian copula. Training data from 2018 and 2019 ([Fraunhofer-Institut für Solare Energiesysteme ISE, 2022](#)). Results generated with all conditional inputs.